ACS Energy LETTERS

http://pubs.acs.org/journal/aelccp

Improved Li^+ Transport in Polyacetal Electrolytes: Conductivity and Current Fraction in a Series of Polymers

Rachel L. Snyder,[#] Youngwoo Choo,[#] Kevin W. Gao, David M. Halat, Brooks A. Abel, Siddharth Sundararaman, David Prendergast, Jeffrey A. Reimer, Nitash P. Balsara,[*] and Geoffrey W. Coates[*]

Cite This: *ACS Energy Lett.* 2021, 6, 1886−1891

Read Online

ACCESS | Metrics & More | Article Recommendations | Supporting Information

ABSTRACT: Polymer electrolytes mitigate safety concerns surrounding flammable liquid electrolytes in lithium-ion batteries. Poly(ethylene oxide) (PEO) electrolytes demonstrate viable conductivity values (~1 × 10^{-3} S/cm) at elevated temperatures (>70 °C) but a relatively low Li^+ current fraction (≤0.2) because strong Li^+ coordination inhibits cation mobility. We have developed a series of polyacetal electrolytes by systematically varying methylene oxide (MO) and ethylene oxide (EO) units in the polymer backbone. These materials maintain high oxygen-to-carbon ratios like PEO but offer improved ion transport, revealing trends of decreasing conductivity and increasing current fraction with respect to polymer composition. In particular, the increasing current fraction measured via the Bruce−Vincent method suggests that MO units improve Li^+ mobility relative to anion mobility. We calculate an overall efficacy (product of conductivity and current fraction) for each polymer/salt composition and identify two polymers—P(EO-MO) and P(EO-2MO)—that outperform PEO at high and low salt concentrations, respectively.

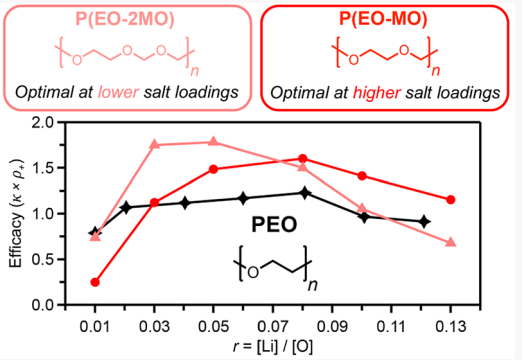

Lithium-ion batteries (LIBs) have dominated commercial energy storage technology since their introduction in the 1970s, largely due to their high energy and power densities.[1,2] The majority of these devices contain low-viscosity liquid electrolytes wherein Lewis basic (i.e., oxygen containing) molecules solvate Li^+ species, forming coordination spheres that can rapidly diffuse and migrate between electrodes.[3,4] Although liquid electrolytes have enabled LIBs with high conductivities, they present significant safety concerns due to their flammability. Over the past 40 years, polymer electrolytes have emerged as safer alternative electrolytes for LIBs.[5] Much of polymer electrolyte development has translated the Lewis basic oxygen-binding motif used for liquid electrolytes to polymeric materials. Poly(ethylene oxide) (PEO) doped with a lithium salt has remained the predominant polymer electrolyte due to its moderate performance, low commercial cost, low toxicity, and good stability.[6] With a high concentration of oxygen relative to carbon, PEO can solvate high concentrations of lithium salts; however, it suffers from inherently low ionic conductivity at room temperature.[7,8] Unlike in liquid electrolytes, oxygens in PEO are covalently linked by the polymer backbone, and Li^+ must inter- or intramolecularly "hop" between coordination environments in a mechanism modulated by relatively slow segmental motion.[9−12]

Polyacetals are a class of polymers that, like PEO, possess a high oxygen-to-carbon ratio, providing both good lithium salt solvation and well-connected binding pathways for lithium transport.[9,13,14] Previous studies have reported promising ion transport properties in polyacetal electrolytes based on poly(1,3-dioxolane) (P(EO-MO))[15−20] and poly(1,3,6-trioxocane) (P(2EO-MO))[21]—wherein the backbone consists of ethylene oxide (EO) and methylene oxide (MO) units. In this study, we developed a series of five polyacetals by systematically varying the EO-to-MO content in the monomers and resultant polymers (Scheme 1). We measured two ion transport parameters in the presence of an applied direct current (dc) potential as found in LIBs—ionic conductivity

Received: March 19, 2021
Accepted: April 19, 2021
Published: April 26, 2021

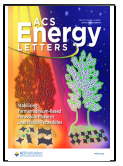

Scheme 1. Generic Polymerization Scheme for the Cationic Ring-Opening Polymerization of Cyclic Acetals (Top Left), Structure of LiTFSI Salt and Salt Loadings (r = [Li]/[O]) Used in This Study (Top Right), and Structures of PEO and the Polyacetals Used in This Study Arranged by Increasing Oxygen-to-Carbon Ratio (p = [O]/[C]) (Bottom)

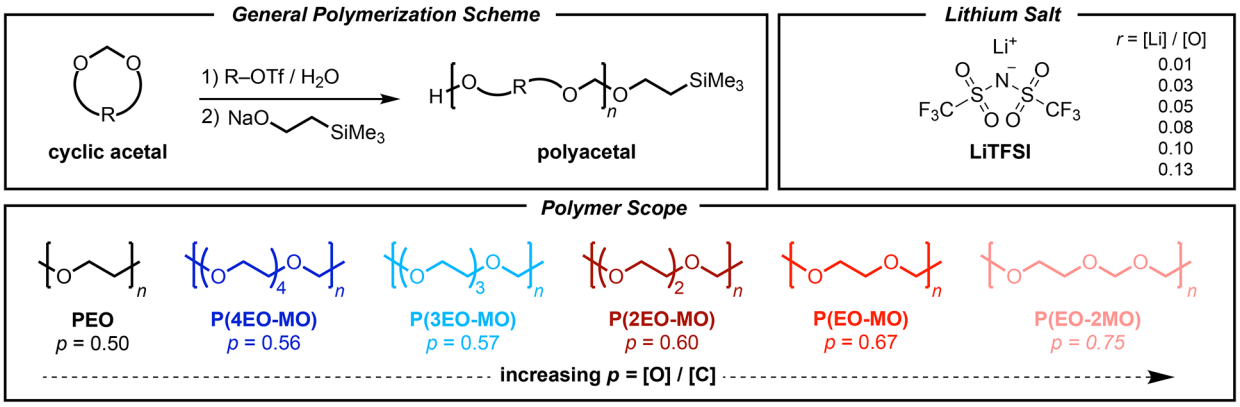

(κ) and cationic current fraction (the fraction of the current carried by Li^+; ρ_+)—as a function of salt concentration in our series of polyacetals. In order to study the relationship between polymer structure and ion transport, we compare both metrics at a given salt concentration with respect to the stoichiometric ratio of oxygen to carbon present in the polymer backbone (p = [O]/[C]). We then calculate the efficacy ($\kappa\rho_+$) of each composition, which is proportional to the steady-state current reached in different electrolytes in the limit of small applied potentials. By examining the dependence of $\kappa\rho_+$ on p, we identify optimal polyacetal electrolyte compositions for ion transport and confirm their promise as polymer electrolytes using cyclic voltammetry.

Polyacetals are typically synthesized via acid-catalyzed cationic ring-opening polymerization (CROP) of cyclic methylene acetals (CAs). We first synthesized the monomers 1,3,5-trioxepane (EO-2MO), 1,3,6-trioxocane (2EO-MO), 1,3,6,9-tetraoxacycloundecane (3EO-MO), and 1,3,6,9,12-pentaoxacyclotetradecane (4EO-MO) from their corresponding diols and paraformaldehyde in the presence of an acid catalyst. 1,3-Dioxolane (EO-MO) was purchased. Using a triflic-acid-based initiator, we polymerized the CA monomer scope to their corresponding polyacetals, terminated the reaction with a soluble alkoxide quenching agent, and employed a thorough purification procedure to give excellent thermal stability of the resultant materials. Detailed synthetic procedures are included in the Supporting Information.

The polyacetals poly(1,3,5-trioxepane) (P(EO-2MO)), poly(1,3-dioxolane) (P(EO-MO)), poly(1,3,6-trioxocane) (P(2EO-MO)), poly(1,3,6,9-tetraoxacycloundecane) (P(3EO-MO)), and poly(1,3,6,9,12-pentaoxacyclotetradecane) (P(4EO-MO)) demonstrated monomodal gel permeation chromatography (GPC) traces with number-average molecular weight (M_n) = 5.2−55.2 kDa (Figure S1). Differential scanning calorimetry (DSC) was used to measure T_g values of −66, −64, −62, −63, and −67 °C for P(EO-2MO), P(EO-MO), P(2EO-MO), P(3EO-MO), and P(4EO-MO), respectively. All polyacetals except P(3EO-MO) were semicrystalline in the neat state with melting temperatures (T_m) ranging from 28−57 °C (Figures S2−S6). Thermogravimetric analysis (TGA) of the neat polyacetals shows excellent thermal stability for all polymers with degradation temperatures at 5% mass loss ($T_{d,5\%}$) >266 °C in all cases (Figure S7).

Each polyacetal was doped with several concentrations of lithium bis(trifluoromethanesulfonyl)imide (LiTFSI) by forming a homogeneous polymer/salt solution in acetonitrile, then removing the solvent and thoroughly drying the samples. When preparing the samples, we designated salt concentration as the molar ratio of lithium ions to oxygen atoms in each polymer (r = [Li]/[O]). This convention is commonly used in PEO-based electrolytes to normalize the lithium concentration to the number of oxygen-binding sites in different polymer compositions. We note that the weight percent (wt %) of LiTFSI at a given r value is different for each polyacetal electrolyte in our series, but this difference is small (<5 wt %) in all cases (Figure S8). Ion transport data for the polyacetal electrolytes with respect to wt % added salt are included in the Supporting Information (Figures S10−S11). In the presence of LiTFSI, the degradation temperature of P(2EO-MO) (and presumably all other polyacetals) decreases, suggesting that LiTFSI facilitates the depolymerization of polyacetals at elevated temperatures (Figure S9). However, $T_{d,5\%}$ values with added salt remain well above the temperature used for electrochemical characterization (90 °C), suggesting these materials maintain excellent thermal stability during use.

We measured the ionic conductivities of the polyacetal electrolytes using electrochemical impedance spectroscopy (EIS). Data were recorded at an elevated temperature (90 °C) to ensure all polymer electrolytes were fully amorphous. The ionic conductivity of each polyacetal electrolyte was measured at salt concentrations from r = 0.01 to 0.13 (Figure 1a). With increasing salt concentration, all polymer electrolytes show expected non-monotonic behavior, wherein there is an initial increase in conductivity to a maximum value followed by a decrease. Increasing conductivity in the dilute regime is expected as the number of charge carriers increases. At higher salt concentrations, the segmental motion is inhibited by the increased number of intermolecular interactions, resulting in lower conductivities.[22] All five polyacetal compositions exhibit peak conductivity values at r = 0.05, which is slightly lower than PEO which peaks at r = 0.08. The observed changes in conductivity are unrelated to differences in polymer molecular weight. As previously reported, PEO electrolytes show comparable ionic conductivities above an entanglement threshold molecular weight of 4 kDa.[23,24] Additionally, P(2EO-MO) shows similar conductivity values at both 20 kDa and 55 kDa (Figure S12). Because the M_n values of the

https://doi.org/10.1021/acsenergylett.1c00594
ACS Energy Lett. 2021, 6, 1886−1891

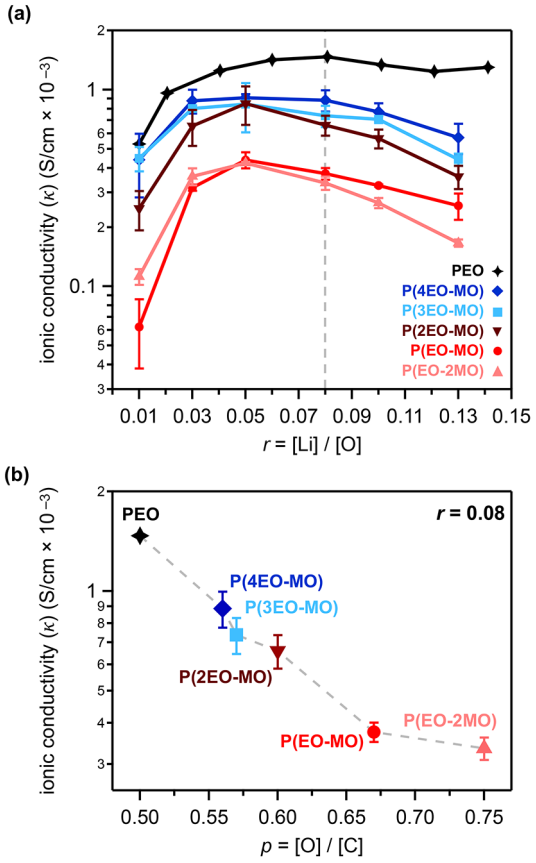

Figure 1. (a) Ionic conductivity measured as a function of salt concentration (r = [Li]/[O]). The conductivity initially increases until reaching an optimal salt concentration, after which it decreases in all cases. (b) Ionic conductivity as a function of polymer composition (p = [O]/[C]) at a single salt concentration of r = 0.08 shows that the conductivity decreases with increasing acetal content.

polyacetals in this work are within the range 4−55 kDa, the effect of molecular weight on ion transport properties is considered to be negligible.

To examine the effect of polymer composition (p = [O]/[C]) on κ, ionic conductivities were compared at a fixed salt concentration of r = 0.08 (Figure 1b). With increasing p, κ values drop by nearly a factor of 4 across the series. Conductivity values are closely tied to segmental relaxation in polymer electrolytes.[12] Relative segmental relaxation in a polymer is typically estimated by the glass transition temperature (T_g). In the presence of LiTFSI, polyacetals show high T_g values as compared to PEO (Table S2). For example, at r = 0.08, PEO has a T_g value of −44 °C, while polyacetals exhibit T_g values of −22, −23, −16, −27, and −31 °C for P(EO-2MO), P(EO-MO), P(2EO-MO), P(3EO-MO), and P(4EO-MO), respectively (Figure S13, Table S2). At 90 °C, the reduced temperature ($T-T_g$, where T = 90 °C) of the polymer electrolytes generally decreases with increasing p = [O]/[C], suggesting slower segmental relaxation in electrolytes with high p values at 90 °C. Therefore, we attribute the decreasing ionic conductivity to decreased segmental relaxation observed in polyacetals[12] as compared to PEO, though additional contributing factors such as polymer polarity[25,26] also play a role.

The current fraction is a measure of the mobility of cations relative to anions in the presence of an applied dc potential. We used Li/electrolyte/Li symmetric cells at 90 °C to measure ρ_+ via the Bruce−Vincent method such that ρ_+ is defined as

$$\rho_+ = \frac{i_{ss}}{i_\Omega}\frac{(\Delta V - i_\Omega R_{i,0}A)}{(\Delta V - i_{ss}R_{i,ss}A)} \quad (1)$$

where i_{ss} and i_Ω refer to the steady-state and initial current densities, respectively, and ΔV is the dc potential across the electrolyte. $R_{i,ss}$ and $R_{i,0}$ are the interfacial impedances at steady state and initial state, respectively, and A is the electrode area. The initial and steady-state interfacial impedances were largely the same, indicating the interfaces between the polyacetal electrolytes and lithium metal electrodes were electrochemically stable for the duration of the measurements. Figure 2a

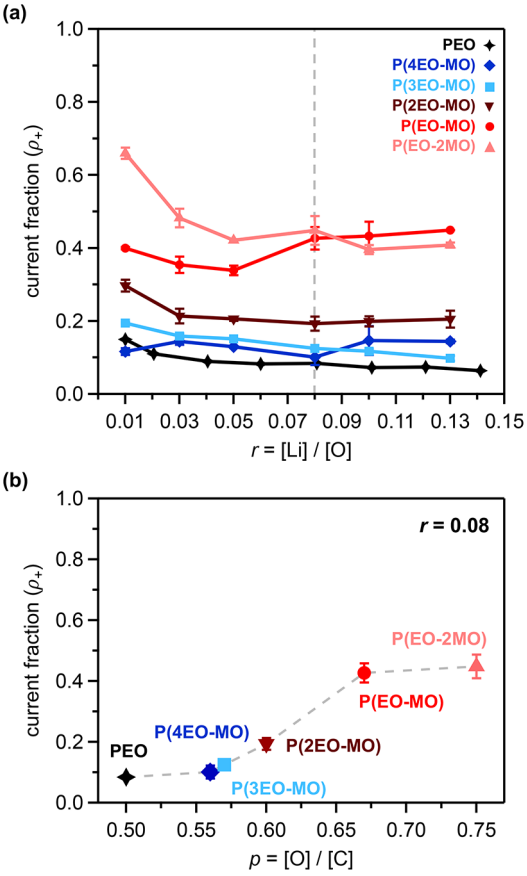

Figure 2. (a) Current fraction (ρ_+) of PEO and the polyacetal series as a function of salt concentration (r = [Li]/[O]). In most cases, the current fraction initially decreases with increasing salt loading, followed by a plateau. The current fraction of P(EO-MO) increases with increasing salt concentration. (b) Current fraction as a function of polymer composition (p = [O]/[C]) at a constant salt concentration of r = 0.08. The current fraction increases with increasing p, suggesting that acetals allow improved cation transport relative to anion transport.

shows the current fraction with respect to the salt concentration in various polyacetal electrolytes as calculated by eq 1. In most cases, ρ_+ decreases as r increases from 0.01 to 0.05. At higher salt concentrations (r > 0.05), the ρ_+ values for PEO, P(4EO-MO), P(3EO-MO), and P(2EO-MO) reach a plateau. P(EO-MO) shows increasing ρ_+ at higher salt

https://doi.org/10.1021/acsenergylett.1c00594
ACS Energy Lett. 2021, 6, 1886−1891

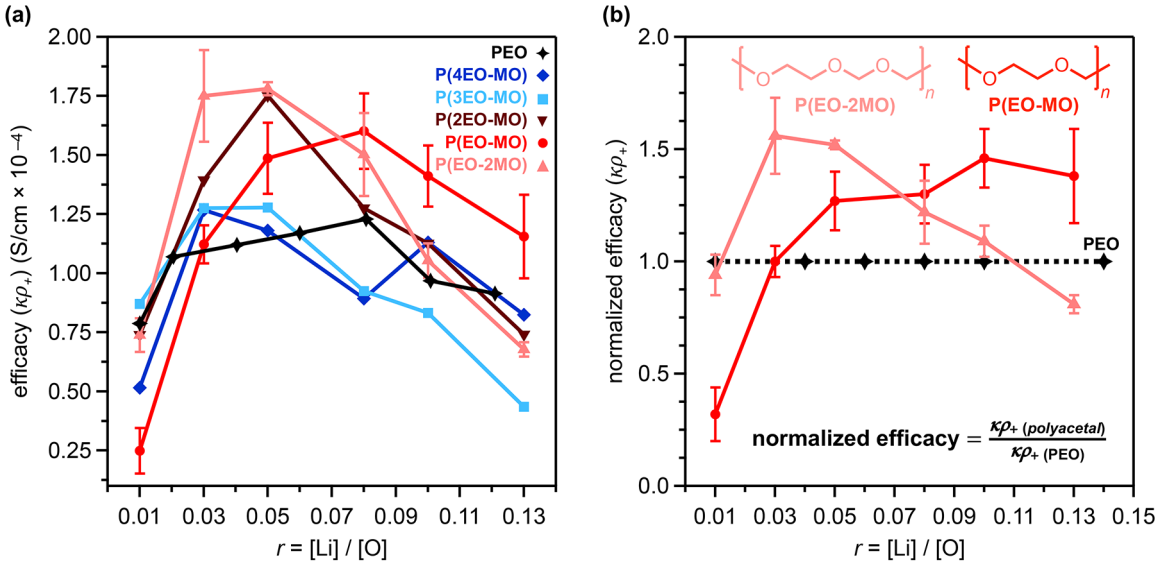

Figure 3. (a) Polymer efficacy at a given salt concentration calculated as the product of conductivity and current fraction. The most efficacious polymer is dependent on salt concentration: P(EO-2MO) shows the best efficacy at lower salt loadings, while P(EO-MO) is most efficacious at higher salt loadings. Some error bars are omitted here for clarity and can be found in the Supporting Information (Figure S14, Tables S4−S8). (b) Efficacy values normalized to those of PEO for the highest performing polyacetals, P(EO-2MO) and P(EO-MO), showing that at most salt concentrations these systems outperform PEO with both polymers showing approximately 1.5 times higher efficacy than PEO at lower salt concentrations (P(EO-2MO)) and high salt concentrations (P(EO-MO)).

concentrations, eventually intersecting with P(EO-2MO). Overall, the current fraction shows an approximately five-fold increase with increasing p value at a fixed salt concentration of r = 0.08 (Figure 2b), reaching values as high as 0.43 and 0.45 for P(EO-MO) and P(EO-2MO), respectively.

Both ionic conductivity and current fraction are important ion transport parameters for evaluating the overall performance of a polymer electrolyte. We therefore calculate the overall efficacy ($\kappa\rho_+$) as the product of conductivity and current fraction at a given salt concentration using the definition of the steady-state current and current fraction obtained by concentrated solution theory:[27]

$$\kappa\rho_+ = \frac{i_{ss}}{\Delta V/L} \tag{2}$$

where L is the distance between the electrodes. As shown in eq 2, the efficacy of the electrolyte at steady-state under a small polarization can be used to represent electrolyte performance under typical operating conditions. Full averaged values and standard deviations are included in the Supporting Information (Figure S14; Tables S3−S8).

The overall $\kappa\rho_+$ of polyacetal electrolytes varies significantly with the salt concentration (Figure 3a). Between r = 0.01 and 0.13, all polyacetal electrolytes demonstrate a peak efficacy value, which appears at lower salt concentrations of r = 0.03−0.05 for P(4EO-MO), P(3EO-MO), P(2EO-MO), and P(EO-2MO). Meanwhile, P(EO-MO) and PEO show optimal $\kappa\rho_+$ at a slightly higher salt concentration of r = 0.08. Although P(4EO-MO) and P(3EO-MO) have efficacies comparable to that of PEO, we have identified three polyacetals that demonstrate enhanced efficacy over PEO: P(2EO-MO), P(EO-MO), and P(EO-2MO). In particular, P(EO-MO) and P(EO-2MO) show the highest efficacy values in higher and lower salt concentration regimes, respectively.

To directly compare the efficacy values of P(EO-MO) and P(EO-2MO) to PEO, we calculated normalized efficacy as a function of p, wherein the efficacy values for P(EO-MO) and P(EO-2MO) were normalized to the efficacy of PEO at a given salt concentration (Figure 3b). In the dilute regime (r = 0.03−0.05), P(EO-2MO) shows the highest efficacy of all studied compositions, over 1.5 times higher than that of PEO. This high efficacy value results from the exceptional ρ_+ of P(EO-2MO) at low salt concentrations (ρ_+ = 0.48) despite relatively low conductivity. At a moderate salt concentration (r = 0.08), both P(EO-MO) and P(EO-2MO) show much improved efficacies approximately 1.3 times higher than that of PEO. P(EO-MO) outcompetes PEO at high salt concentrations (r = 0.10−0.13), demonstrating efficacy values nearly 1.4 times higher than those of PEO; its uniquely increasing ρ_+ with increasing salt concentration is largely responsible for the high efficacy values. Since practical electrolytes contain high salt concentrations, P(EO-MO) is the best polymer electrolyte candidate identified in this work.

Both P(EO-MO) and P(EO-2MO) show a wide electrochemical stability window as measured by cyclic voltammetry (Figures S16−S17, data obtained at a sweep rate of 1 mV/s). The voltammetric profiles are shown for cycle 15, demonstrating the stabilized current profiles. The initial cycles exhibit increased currents during the formation of the solid electrolyte interface. At both r = 0.05 and r = 0.08, P(EO-2MO) shows excellent voltage stability and expected redox behavior with current densities comparable to those observed in PEO (Figure S16). In the presence of LiTFSI, P(EO-MO) shows a higher current density at low potentials at both r = 0.08 and r = 0.10, suggesting the observed current may arise from either a salt or polymer degradation reaction, although more in-depth studies are needed to investigate further (Figure S17). Nevertheless, both polyacetals show promising electrochemical stability windows similar to that of PEO, validating their potential application in commercial LIBs.

In summary, we systematically studied two ion transport parameters across a series of polyacetal electrolytes and PEO at

https://doi.org/10.1021/acsenergylett.1c00594
ACS Energy Lett. 2021, 6, 1886−1891

varying salt concentrations and identified trends in ion mobility with polymer composition. With increasing p = [O]/[C], we see a four-fold decrease in ionic conductivity, likely related to changes in segmental motion. However, the current fraction advantageously increases up to a factor of 5 with increasing oxygen content. Although the conductivity is sacrificed with increasing oxygen content, the current fraction compensates for the decreased conductivity. Resolving these two trends by calculating electrolyte efficacy ($\kappa\rho_+$), we identify several optimal polyacetal compositions that outperform PEO, including P(EO-2MO) which shows the highest overall efficacy at lower salt concentrations, and P(EO-MO) which exhibits excellent efficacy at high salt concentrations. Both P(EO-2MO) and P(EO-MO) have wide electrochemical stability windows, rendering them viable candidates for PEO-replacement polymer electrolytes.[28] The observations presented here provide a pathway to move past PEO polymer electrolytes that have dominated the field since 1973.

■ ASSOCIATED CONTENT

Supporting Information

The Supporting Information is available free of charge at https://pubs.acs.org/doi/10.1021/acsenergylett.1c00594.

Monomer and polymer syntheses, neat polymer characterization, electrochemical experimental procedures, and additional electrochemical data (PDF)

■ AUTHOR INFORMATION

Corresponding Authors

Geoffrey W. Coates − *Department of Chemistry and Chemical Biology, Baker Laboratory, Cornell University, Ithaca, New York 14853, United States; Joint Center for Energy Storage Research, Argonne National Laboratory, Lemont, Illinois 60439, United States;* orcid.org/0000-0002-3400-2552; Email: coates@cornell.edu

Nitash P. Balsara − *Joint Center for Energy Storage Research, Argonne National Laboratory, Lemont, Illinois 60439, United States; Materials Sciences Division, Lawrence Berkeley National Laboratory, Berkeley, California 94720, United States; Department of Chemical and Biomolecular Engineering and College of Chemistry, University of California, Berkeley, California 94720, United States;* orcid.org/0000-0002-0106-5565; Email: nbalsara@berkeley.edu

Authors

Rachel L. Snyder − *Department of Chemistry and Chemical Biology, Baker Laboratory, Cornell University, Ithaca, New York 14853, United States; Joint Center for Energy Storage Research, Argonne National Laboratory, Lemont, Illinois 60439, United States;* orcid.org/0000-0002-0569-0704

Youngwoo Choo − *Joint Center for Energy Storage Research, Argonne National Laboratory, Lemont, Illinois 60439, United States; Materials Sciences Division, Lawrence Berkeley National Laboratory, Berkeley, California 94720, United States;* orcid.org/0000-0003-2715-0618

Kevin W. Gao − *Joint Center for Energy Storage Research, Argonne National Laboratory, Lemont, Illinois 60439, United States; Materials Sciences Division, Lawrence Berkeley National Laboratory, Berkeley, California 94720, United States; Department of Chemical and Biomolecular Engineering and College of Chemistry, University of California, Berkeley, California 94720, United States;* orcid.org/0000-0002-6794-1265

David M. Halat − *Joint Center for Energy Storage Research, Argonne National Laboratory, Lemont, Illinois 60439, United States; Materials Sciences Division, Lawrence Berkeley National Laboratory, Berkeley, California 94720, United States; Department of Chemical and Biomolecular Engineering and College of Chemistry, University of California, Berkeley, California 94720, United States;* orcid.org/0000-0002-0919-1689

Brooks A. Abel − *Department of Chemistry and Chemical Biology, Baker Laboratory, Cornell University, Ithaca, New York 14853, United States; Joint Center for Energy Storage Research, Argonne National Laboratory, Lemont, Illinois 60439, United States;* orcid.org/0000-0002-2288-1975

Siddharth Sundararaman − *Joint Center for Energy Storage Research, Argonne National Laboratory, Lemont, Illinois 60439, United States; The Molecular Foundry, Lawrence Berkeley National Laboratory, Berkeley, California 94720, United States*

David Prendergast − *Joint Center for Energy Storage Research, Argonne National Laboratory, Lemont, Illinois 60439, United States; The Molecular Foundry, Lawrence Berkeley National Laboratory, Berkeley, California 94720, United States;* orcid.org/0000-0003-0598-1453

Jeffrey A. Reimer − *Joint Center for Energy Storage Research, Argonne National Laboratory, Lemont, Illinois 60439, United States; Materials Sciences Division, Lawrence Berkeley National Laboratory, Berkeley, California 94720, United States; Department of Chemical and Biomolecular Engineering and College of Chemistry, University of California, Berkeley, California 94720, United States;* orcid.org/0000-0002-4191-3725

Complete contact information is available at: https://pubs.acs.org/10.1021/acsenergylett.1c00594

Author Contributions

[#]R.L.S. and Y.C. contributed equally. All other authors contributed equally and have given approval to the final version of the manuscript.

Notes

The authors declare no competing financial interest.

■ ACKNOWLEDGMENTS

This work was fully supported by the Joint Center for Energy Storage Research (JCESR), an Energy Innovation Hub funded by the U.S. Department of Energy, Office of Science, Basic Energy Sciences. Work at the Molecular Foundry was supported by the Office of Science, Office of Basic Energy Sciences, of the U.S. Department of Energy under Contract No. DE-AC02-05CH11231. We thank Dr. Ivan Keresztes at Cornell University for his help with the NMR analysis of P(EO-2MO). This work made use of the Cornell Center for Materials Research and the NMR Facility at Cornell University, which are supported by the NSF under Awards DMR-1719875 and CHE-1531632, respectively. K.W.G. acknowledges funding from a National Defense Science and Engineering Fellowship.

■ REFERENCES

(1) Goodenough, J. B.; Park, K.-S. The Li-Ion Rechargeable Battery: A Perspective. *J. Am. Chem. Soc.* **2013**, *135*, 1167−1176.

(2) Trahey, L.; Brushett, F. R.; Balsara, N. P.; Ceder, G.; Cheng, L.; Chiang, Y.-M.; Hahn, N. T.; Ingram, B. J.; Minteer, S. D.; Moore, J. S.; Mueller, K. T.; Nazar, L. F.; Persson, K. A.; Siegel, D. J.; Xu, K.; Zavadil, K. R.; Srinivasan, V.; Crabtree, G. W. Energy Storage Emerging: A Perspective from the Joint Center for Energy Storage Research. *Proc. Natl. Acad. Sci. U. S. A.* **2020**, *117*, 12550−12557.
(3) Xu, K. Nonaqueous Liquid Electrolytes for Lithium-Based Rechargeable Batteries. *Chem. Rev.* **2004**, *104*, 4303−4418.
(4) Choo, Y.; Halat, D. M.; Villaluenga, I.; Timachova, K.; Balsara, N. P. Diffusion and Migration in Polymer Electrolytes. *Prog. Polym. Sci.* **2020**, *103*, 101220.
(5) Zhang, H.; Li, C.; Piszcz, M.; Coya, E.; Rojo, T.; Rodriguez-Martinez, L. M.; Armand, M.; Zhou, Z. Single Lithium-Ion Conducting Solid Polymer Electrolytes: Advances and Perspectives. *Chem. Soc. Rev.* **2017**, *46*, 797−815.
(6) Manthiram, A.; Yu, X.; Wang, S. Lithium Battery Chemistries Enabled by Solid-State Electrolytes. *Nat. Rev. Mater.* **2017**, *2*, 16103.
(7) Tarascon, J.-M.; Armand, M. Issues and Challenges Facing Rechargeable Lithium Batteries. *Nature* **2001**, *414*, 359−367.
(8) Fenton, D. E.; Parker, J. M.; Wright, P. V. Complexes of Alkali Metal Ions with Poly(Ethylene Oxide). *Polymer* **1973**, *14*, 589.
(9) Ratner, M. A.; Johansson, P.; Shriver, D. F. Polymer Electrolytes: Ionic Transport Mechanisms and Relaxation Coupling. *MRS Bull.* **2000**, *25*, 31−37.
(10) Armand, M. Polymers with Ionic Conductivity. *Adv. Mater.* **1990**, *2*, 278−286.
(11) Bresser, D.; Lyonnard, S.; Iojoiu, C.; Picard, L.; Passerini, S. Decoupling Segmental Relaxation and Ionic Conductivity for Lithium-Ion Polymer Electrolytes. *Mol. Syst. Des. Eng.* **2019**, *4*, 779−792.
(12) Schauser, N. S.; Nikolaev, A.; Richardson, P. M.; Xie, S.; Johnson, K.; Susca, E. M.; Wang, H.; Seshadri, R.; Clément, R. J.; Read de Alaniz, J.; Segalman, R. A. Glass Transition Temperature and Ion Binding Determine Conductivity and Lithium−Ion Transport in Polymer Electrolytes. *ACS Macro Lett.* **2021**, *10*, 104−109.
(13) Borodin, O.; Smith, G. D. Mechanism of Ion Transport in Amorphous Poly(Ethylene Oxide)/LiTFSI from Molecular Dynamics Simulations. *Macromolecules* **2006**, *39*, 1620−1629.
(14) Webb, M. A.; Jung, Y.; Pesko, D. M.; Savoie, B. M.; Yamamoto, U.; Coates, G. W.; Balsara, N. P.; Wang, Z.-G.; Miller, T. F., III Systematic Computational and Experimental Investigation of Lithium-Ion Transport Mechanisms in Polyester-Based Polymer Electrolytes. *ACS Cent. Sci.* **2015**, *1*, 198−205.
(15) Silva, R. A.; Goulart Silva, G.; Furtado, C. A.; Moreira, R. L.; Pimenta, M. A. Structure and Conductivity in Polydioxolane/$LiCF_3SO_3$ Electrolytes. *Electrochim. Acta* **2001**, *46*, 1493−1498.
(16) Goulart, G.; Sanchez, J.-Y.; Armand, M. Synthesis and Electrochemical Characterization of New Polymer Electrolytes Based on Dioxolane Homo and Co-Polymers. *Electrochim. Acta* **1992**, *37*, 1589−1592.
(17) Zhou, J.; Qian, T.; Liu, J.; Wang, M.; Zhang, L.; Yan, C. High-Safety All-Solid-State Lithium-Metal Battery with High-Ionic-Conductivity Thermoresponsive Solid Polymer Electrolyte. *Nano Lett.* **2019**, *19*, 3066−3073.
(18) Zhao, Q.; Liu, X.; Stalin, S.; Khan, K.; Archer, L. A. Solid-State Polymer Electrolytes with in-Built Fast Interfacial Transport for Secondary Lithium Batteries. *Nat. Energy* **2019**, *4*, 365−373.
(19) Khan, K.; Tu, Z.; Zhao, Q.; Zhao, C.; Archer, L. A. Synthesis and Properties of Poly-Ether/Ethylene Carbonate Electrolytes with High Oxidative Stability. *Chem. Mater.* **2019**, *31*, 8466−8472.
(20) Liu, F.-Q.; Wang, W.-P.; Yin, Y.-X.; Zhang, S.-F.; Shi, J.-L.; Wang, L.; Zhang, X.-D.; Zheng, Y.; Zhou, J.-J.; Li, L.; Guo, Y.-G. Upgrading Traditional Liquid Electrolyte via *in Situ* Gelation for Future Lithium Metal Batteries. *Sci. Adv.* **2018**, *4*, eaat5383.
(21) Zheng, Q.; Pesko, D. M.; Savoie, B. M.; Timachova, K.; Hasan, A. L.; Smith, M. C.; Miller, T. F., III; Coates, G. W.; Balsara, N. P. Optimizing Ion Transport in Polyether-Based Electrolytes for Lithium Batteries. *Macromolecules* **2018**, *51*, 2847−2858.
(22) Mongcopa, K. I. S.; Tyagi, M.; Mailoa, J. P.; Samsonidze, G.; Kozinsky, B.; Mullin, S. A.; Gribble, D. A.; Watanabe, H.; Balsara, N. P. Relationship between Segmental Dynamics Measured by Quasi-Elastic Neutron Scattering and Conductivity in Polymer Electrolytes. *ACS Macro Lett.* **2018**, *7*, 504−508.
(23) Teran, A. A.; Tang, M. H.; Mullin, S. A.; Balsara, N. P. Effect of Molecular Weight on Conductivity of Polymer Electrolytes. *Solid State Ionics* **2011**, *203*, 18−21.
(24) Devaux, D.; Bouchet, R.; Glé, D.; Denoyel, R. Mechanism of Ion Transport in PEO/LiTFSI Complexes: Effect of Temperature, Molecular Weight and End Groups. *Solid State Ionics* **2012**, *227*, 119−127.
(25) Wheatle, B. K.; Fuentes, E. F.; Lynd, N. A.; Ganesan, V. Influence of Host Polarity on Correlating Salt Concentration, Molecular Weight, and Molar Conductivity in Polymer Electrolytes. *ACS Macro Lett.* **2019**, *8*, 888−892.
(26) Wheatle, B. K.; Lynd, N. A.; Ganesan, V. Effect of Polymer Polarity on Ion Transport: A Competition between Ion Aggregation and Polymer Segmental Dynamics. *ACS Macro Lett.* **2018**, *7*, 1149−1154.
(27) Galluzzo, M. D.; Maslyn, J. A.; Shah, D. B.; Balsara, N. P. Ohm's Law for Ion Conduction in Lithium and beyond-Lithium Battery Electrolytes. *J. Chem. Phys.* **2019**, *151*, 020901.
(28) Mindemark, J.; Lacey, M. J.; Bowden, T.; Brandell, D. Beyond PEO—Alternative Host Materials for Li^+-Conducting Solid Polymer Electrolytes. *Prog. Polym. Sci.* **2018**, *81*, 114−143.

https://doi.org/10.1021/acsenergylett.1c00594
ACS Energy Lett. 2021, 6, 1886−1891